Extremum Seeking Control for Power Tracking via Functional Electrical Stimulation ⋆

Victor H. Duenas * **Christian A. Cousin** *
Courtney A. Rouse * **Warren E. Dixon** *

* *Department of Mechanical and Aerospace Engineering, University of Florida, Gainesville, USA (e-mail: {vhduenas, ccousin, courtneyarouse, wdixon}@ufl.edu).*

Abstract: Motorized Functional Electrical Stimulation (FES)-cycling is a promising rehabilitative strategy for people possessing movement disorders as a result of neurological conditions. Cadence and torque (power) tracking objectives have been previously prescribed in FES-cycling to exploit the functional benefits of neuromuscular electric stimulation and produce intensive active therapy with motorized assistance. However, predetermined desired trajectories for either objective may yield sub-optimal training performance since the movement capacity of a person recovering from injury is unknown and time-varying. Hence, online adaptation is well-motivated to determine optimal cadence and torque trajectories. In this paper, an extremum seeking control (ESC) algorithm is implemented in real-time to compute the optimal cadence and torque trajectory (i.e., the peak torque demand) to maximize power output in an FES-cycling protocol. The uncertain, nonlinear FES-cycle system is an autonomous, state-dependent switched system to activate lower-limb muscles and an electric motor. Torque tracking is achieved by electrically stimulating the muscles via a learning controller and cadence tracking by engaging an electric motor. A passivity-based approach is utilized to analyze the stability of both tracking objectives. Experimental testing was performed on one able-bodied individual to demonstrate the feasibility of the control development.

Keywords: Extremum Seeking Control (ESC), Functional Electrical Stimulation (FES) Cycling, Repetitive Learning Control (RLC), Passivity-Based Control

1. INTRODUCTION

Rehabilitative technologies based on functional electrical stimulation (FES) allow people with movement disorders to engage in activities that promote motor learning and functional improvements Nataraj et al. (2017). Lower-limb FES-cycling has been recommended as a rehabilitative strategy for cardiovascular training of post-stroke participants and individuals with spinal cord injuries Sadowsky et al. (2013); Ferrante et al. (2008); Bo et al. (2017). Rehabilitation protocols that involve motorized cycles with FES have provided means to exercise lower-limb muscles and achieve consistent, repetitive movements with the assistance of an electric motor. Closed-loop control strategies have been implemented for cadence tracking, utilizing feedback control with identification procedures Hunt et al. (2004), robust methods to compensate for the nonlinear, time-varying rider-cycle dynamics Bellman et al. (2016, 2017), repetitive learning control (RLC) to exploit the inherent periodic nature of cycling Duenas et al. (2016, to appear), and the activation of biarticular muscles Kawai et al. (to appear). Simultaneous control of cadence and torque is another common task specific to FES-cycling. Power (i.e., torque) tracking protocols seek to enhance cardiopulmonary and muscular gains (i.e., metabolic demand) and accelerate movement recovery Szecsi et al. (2014). Previous results have addressed the objective of power tracking in FES-cycling, utilizing robust control methods and switched control strategies Farhoud and Erfanian (2014); Cousin et al. (2017); Bellman (2015).

Motorized FES-cycles have the capability to regulate cadence and vary the resistive load to evoke torque from the rider. The design of high-level controllers to determine the desired kinematic and torque trajectories for lower-limb tasks have been based on time, joint angles, and electromyographic measurements Zhang et al. (2015). However, the use of arbitrary cadence and torque trajectories usually demonstrate limited effectiveness due to the lack of sufficient knowledge about the human's motor capability during rehabilitation. Hence, there is a growing need for cyber-physical-human-oriented rehabilitation protocols Beckerle et al. (2017) such as motorized FES-cycling. Moreover, since people with movement disorders possess different levels of residual neurological motor control, the use of predetermined desired trajectories in cycling has the potential to yield suboptimal exercise training per-

⋆ This research is supported in part by the National Science Foundation Graduate Research Fellowship Program under Grant No. DGE-1315138 and AFOSR award number FA9550-18-1-0109. Any opinions, findings, and conclusions or recommendations expressed in this material are those of the author(s) and do not necessarily reflect the views of the sponsoring agency.

Preprint submitted to 2nd IFAC Conference on Cyber-Physical & Human-Systems.
Received April 23, 2018.

formance (e.g., requiring iterative manual adjustments of the desired cadence or torque trajectories to match the participant's motor capacity). Hence, an online adaptation strategy is well-motivated to determine optimal cadence and torque trajectories during FES-cycling to accommodate for the rider's unique characteristics.

Extremum Seeking Control (ESC) is an adaptive control technique that exploits the existence of an unknown steady state input-to-output mapping with a local (or global) extremum to achieve online optimization for nonlinear dynamical systems. A common ESC method includes the use of a periodic perturbation (i.e., a dither signal) injected in the feedback loop, similar to the persistence of excitation condition, to explore the neighborhood around the setpoint to find the extremum. The first stability proof for the perturbation-based scheme was introduced in Krstic and Wang (2000) and has been extensively used in different applications, such as to tune the gains of a PID controller Killingsworth and Krstic (2006), maximize the human's power output in an upper-arm exercise machine Zhang et al. (2006), control the end effector of a robotic system Koropouli et al. (2016), and design an adaptive cruise control system Rahnama et al. (2016). More recently, novel contributions have been developed for the design and analysis of ESC for hybrid systems Poveda and Teel (2017); Poveda et al. (2017), in combination with iterative learning control Cao et al. (2017), using switching-based strategies Chen et al. (2017); Moura and Chang (2010), and using a distributed approach for optimization among networked agents Ye and Hu (2016).

In the context of FES, few studies have implemented extremum seeking methods Stegath et al. (2007); Oliveira et al. (2016). In Stegath et al. (2007), a numerical extremum seeking method is implemented to find optimal stimulation parameters (e.g., frequency and voltage amplitude) for a leg extension task. In Oliveira et al. (2016), extremum seeking is applied to tune the gains of a PID controller for elbow movements via electrical stimulation of the biceps and triceps brachii. The current paper leverages ESC as an online adaptive method to determine optimal cadence and torque trajectories to maximize power output in FES-cycling.

In this paper, an ESC algorithm inspired by the perturbation-based method Ariyur and Krstic (2003); Krstic and Wang (2000); Zhang et al. (2006) and by the recent contribution of proportional-integral ESC developed in Guay (2016) is developed for a motorized FES-cycling protocol. The objective is to maximize the cycling power output of the rider by modifying the desired power and accommodate for the unique movement capabilities of the rider. Since the maximum power (based on the cadence and the peak torque demand) is unknown and user-dependent, ESC is well-motivated for power tracking in cycling. The extremum seeking adaptation saturates the rider's measured power output to ensure boundedness of the desired trajectories. A switched FES controller with a feedforward learning input is designed to track the desired state-dependent torque trajectory. The shape of the desired torque trajectory is designed based on the knee kinematic effectiveness of the rider (i.e., varies as a function of the crank angle) and the peak torque demand is computed by the ESC. In parallel, a robust sliding-mode cadence controller is designed for the electric motor. The cycle-rider model includes the switching effects of activating multiple muscle groups based on a state-dependent activation pattern that exploits the kinematic effectiveness of the rider. A passivity-based analysis is developed to ensure stability of the torque (muscle control) and cadence (motor control) subsystems. Experimental testing was conducted on a single able-bodied individual for control validation and additional experiments are on-going.

2. STATIONARY CYCLE-RIDER DYNAMIC MODEL WITH SWITCHED INPUTS

The dynamic model of the rider and the cycle with lower-limb muscle and electric motor inputs is given as Bellman et al. (2016)

$$M(q)\ddot{q} + V(q,\dot{q})\dot{q} + G(q) + P(q,\dot{q}) + c_d\dot{q} + d(t) = B_e u_e + B_\sigma u_m, \quad (1)$$

where $q : \mathbb{R}_{\geq t_0} \to \mathcal{Q}$ denotes the measurable crank angle, $\mathcal{Q} \subseteq \mathbb{R}$ denotes the set of crank angles, and $t_0 \in \mathbb{R}$ is the initial time. The combined inertial effects of the rider and the cycle are denoted by $M : \mathcal{Q} \to \mathbb{R}_{>0}$; $V : \mathcal{Q} \times \mathbb{R} \to \mathbb{R}$ and $G : \mathcal{Q} \to \mathbb{R}$ denote the centripetal-Coriolis and gravitational effects, respectively; $P : \mathcal{Q} \times \mathbb{R} \to \mathbb{R}$ denotes the effects of passive viscoelastic tissue forces in the rider's joints; $c_d \in \mathbb{R}_{>0}$ denotes the unknown coefficient of viscous damping in the cycle; $d : \mathbb{R}_{\geq t_0} \to \mathbb{R}$ denotes the uncertain disturbances in the system; $B_e \in \mathbb{R}_{>0}$ is a positive torque constant, which satisfies $B_e \geq c_e \in \mathbb{R}_{>0}$, $u_e : \mathbb{R}_{\geq t_0} \to \mathbb{R}$ is the motor current control input, and $u_m : \mathbb{R}_{\geq t_0} \to \mathbb{R}$ denotes the stimulation intensity applied to each muscle group. The lumped switched control effectiveness, denoted by $B_\sigma \in \mathbb{R}_{\geq 0}$, is defined as

$$B_\sigma(q,\dot{q}) \triangleq \sum_{m \in \mathcal{M}} B_m(q,\dot{q}) k_m \sigma_m(q), \quad (2)$$

where the subscript $\sigma \in \mathcal{P} \triangleq \{1, 2, 3, ...N\}$, $\mathcal{P} \subset \mathbb{N}$, $N \in \mathbb{N}$ indicates the index of B_σ and switches according to the crank position and N represents the total number possible permutations of active muscles. The uncertain control effectiveness of each muscle is denoted by $B_m : \mathcal{Q} \times \mathbb{R} \to \mathbb{R}_{>0}$ with subscript m indicating an element in the muscle set $\mathcal{M}$ (i.e., the stimulated muscle groups), and $k_m \in \mathbb{R}_{>0}$, $\forall m \in \mathcal{M}$ are the selectable positive control gains. The stimulation intensities u_m, $\forall m \in \mathcal{M}$ are applied to the muscle groups in regions of the crank cycle when the torque transfer efficiencies are above a predefined threshold $\varepsilon_m \in [0, 1]$, $\forall m \in \mathcal{M}$. Switching occurs between different muscle groups yielding an autonomous, state-dependent, switched control system. The portion of the crank cycle over which a particular muscle group is stimulated is denoted by $\mathcal{Q}_m \subset \mathcal{Q}$, $\forall m \in \mathcal{M}$, where the muscle groups are activated as described in Bellman et al. (2016) so that $\mathcal{Q}_M \triangleq \bigcup_{m \in \mathcal{M}} \mathcal{Q}_m$. A piecewise constant switching signal can be developed for each muscle group, $\sigma_m \in \{0,\ 1\}$, $\forall m \in \mathcal{M}$ as

$$\sigma_m(q) \triangleq \begin{cases} 1 & \text{if } q \in \mathcal{Q}_m \\ 0 & \text{if } q \notin \mathcal{Q}_m \end{cases}. \quad (3)$$

The known sequence of switching states, which are the limit points of $\mathcal{Q}_m$, $\forall m \in \mathcal{M}$, is defined as $\{q_n\}$,$n \in \{0,\ 1,\ 2,\ ...\}$, and the corresponding sequence of unknown

Preprint submitted to 2nd IFAC Conference on Cyber-Physical & Human-Systems.
Received April 23, 2018.

switching times $\{t_n\}$ is defined such that each t_n denotes the instant when q reaches the corresponding switching state q_n. The switching signal σ_m is designed to produce forward pedaling only. The following assumption and properties of the switched system in (1) will be exploited in the subsequent control design and stability analysis Bellman et al. (2016)

Assumption 1. The disturbance term d is bounded as $|d| \leq \xi_d$, where $\xi_d \in \mathbb{R}_{>0}$ is a known constant.

Property 1. $c_m \leq M \leq c_M$, where c_m, $c_M \in \mathbb{R}_{>0}$ are known constants. **Property 2.** $|V| \leq c_V |\dot{q}|$, where $c_V \in \mathbb{R}_{>0}$ is a known constant. **Property 3.** $|G| \leq c_G$, where $c_G \in \mathbb{R}_{>0}$ is a known constant. **Property 4.** $|P| \leq c_{P1} + c_{P2} |\dot{q}|$, where c_{P1}, $c_{P2} \in \mathbb{R}_{>0}$ are known constants. **Property 5.** $\frac{1}{2}\dot{M} = V$ by skew symmetry. **Property 6.** The lumped switching control effectiveness is bounded as $c_b \leq B_\sigma \leq c_B$, $\forall \sigma \in \mathcal{P}$, where $c_b, c_B \in \mathbb{R}_{>0}$ are known constants.

3. EXTREMUM SEEKING FOR DESIRED TRAJECTORY GENERATION

The desired cadence $\dot{q}_d : \mathbb{R}_{\geq t_0} \to \mathbb{R}$ and the desired torque $\tau_d : \mathbb{R}_{\geq t_0} \to \mathbb{R}$ can be generated using ESC such that $\dot{q}_d$, $\tau_d \in \mathcal{L}_\infty$ and $\dot{q}_d(t) \to \dot{q}_d^*$ and $\tau_d \to \tau_d^*$, where $\dot{q}_d^*$ and τ_d^* are unknown optimal constants that maximize the rider's power output. In practice, the generated desired cadence $\dot{q}_d$ and desired torque τ_d approach a neighborhood of the unknown optimal values. The rider's power output can be expressed as

$$P_a(t) = \tau_a(q, \dot{q}, t)\dot{q}, \tag{4}$$

where $\tau_a : \mathcal{Q} \times \mathbb{R} \times \mathbb{R}_{\geq t_0} \to \mathbb{R}$ is the torque produced by the muscle contractions and is defined as $\tau_a \triangleq B_\sigma u_m$, and $\dot{q} : \mathbb{R}_{\geq t_0} \to \mathbb{R}$ is the computable velocity of the system.

The objective is to develop an adaptive feedback mechanism which maximizes the steady state value of P_a without requiring the explicit knowledge of $\dot{q}_d^*$ or τ_d^*. It is assumed that there exists an unknown maximum power (i.e., P_a^*) evoked by the rider during a cycling protocol. The proof of convergence of the adaptive ESC mechanism is omitted here, but follows from standard singular perturbation analysis Khalil (2002) and averaging techniques as extensively discussed in literature Krstic and Wang (2000); Ariyur and Krstic (2003). Inspired by the perturbation-based approach in Krstic and Wang (2000) and leveraging the recent development in proportional-integral (PI)-ESC in Guay (2016), a saturated extremum-seeking algorithm is developed for generating $\dot{q}_d$ as

$$\begin{aligned}
\dot{q}_d &= \hat{\theta} + \left(\alpha_p - \frac{k_d}{\alpha_p} w\right) \sin(\omega t), \\
\dot{\hat{\theta}} &= -k_\theta w \sin(\omega t), \\
\dot{\nu} &= -\left(k_h \nu + \text{sat}(P_a)\right), \\
w &= -\left(k_h^2 \nu + k_h \text{sat}(P_a)\right),
\end{aligned} \tag{5}$$

where $\alpha_p \in \mathbb{R}_{>0}$ is the positive constant amplitude of the perturbation signal (i.e., dither signal), $\omega \in \mathbb{R}_{>0}$ is the frequency of the perturbation, $k_d, k_\theta, k_h \in \mathbb{R}_{>0}$ are constant design parameters, $\hat{\theta}, \nu, w : \mathbb{R}_{\geq t_0} \to \mathbb{R}$ are auxiliary signals, and $\text{sat}(\cdot)$ is a continuous saturation function defined as

$$\text{sat}_\beta(\cdot) \triangleq \begin{cases} \cdot & \text{for } |\cdot| \leq \beta \\ \text{sgn}(\cdot)\beta & \text{for } |\cdot| > \beta \end{cases}. \tag{6}$$

The use of the saturation function is incorporated to ensure that $\dot{q}_d \in \mathcal{L}_\infty$. The tuning of the parameters α_p, ω, k_d, k_θ, and k_h are selected sufficiently small compared to the selectable controller gains introduced in the following section to ensure that the designed controllers can track the computed trajectories by the ESC algorithm in (5). Moreover, the design of the cadence and torque controllers have to exhibit faster response than the ESC algorithm in (5) to ensure convergence of the tracking errors (i.e., time scale separation between the ESC and closed-loop feedback controllers) Ariyur and Krstic (2003); Zhang et al. (2006). To achieve faster response by the feedback controllers compared to the ESC requires particular attention to the tuning of the ESC parameters in (5). First, the perturbation frequency ω has to be slower than the closed-loop error system decay. For the saturated PI-ESC in (5) and based on Guay (2016, Theorem 2), the gain k_h is recommended to be larger than ω. In addition, the initial condition of ν (i.e., $\nu(t_0)$) is defined as $\nu(t_0) \triangleq \frac{\text{sat}(P_a)}{k_h}$, to avoid a sudden jump for the direct feedthrough term w while computing $\dot{q}_d$ in (5).

Remark 1. The ESC algorithm in (5) is also used to compute the torque trajectory τ_d to maximize power output from the rider.

Remark 2. Alternatively to the perturbation-based ESC approach, several numerical optimization-based algorithms have been implemented in practice as in Zhang and nez (2009); Zhang et al. (2006), which may be suitable for FES-cycling power tracking.

4. CONTROL DEVELOPMENT

4.1 Cadence Control

The first objective is to design a motor controller to track the generated cadence trajectory. To quantify the cadence objective, a cadence-tracking error denoted by $e : \mathbb{R}_{\geq t_0} \to \mathbb{R}$ is defined as

$$e \triangleq \dot{q} - \dot{q}_d. \tag{7}$$

The open-loop cadence error system is obtained by taking the time derivative of (7), multiplying it by M, and substituting (1) as

$$M\dot{e} = -Ve + \chi + B_\sigma u_m + B_e u_e, \tag{8}$$

where the auxiliary signal $\chi : \mathcal{Q} \times \mathbb{R} \times \mathbb{R}_{\geq t_0} \to \mathbb{R}$ is defined as

$$\chi \triangleq -M\ddot{q}_d - V\dot{q}_d - Gq - P - c_d\dot{q} - d. \tag{9}$$

Using Properties 1-4, χ can be upper bounded as

$$|\chi| \leq c_1 + c_2|e|, \tag{10}$$

Preprint submitted to 2nd IFAC Conference on Cyber-Physical & Human-Systems.
Received April 23, 2018.

where $c_1, c_2 \in \mathbb{R}_{>0}$ are known positive constants. Given the open-loop cadence error system in (8), the control input to the motor is designed as

$$u_e \triangleq -k_1 e - k_2 \text{sgn}(e), \tag{11}$$

where $k_1, k_2 \in \mathbb{R}_{>0}$ are selectable positive gain constants and sgn$(\cdot)$ is the signum function. By substituting (11) into (8), the closed-loop cadence error system is obtained as

$$M\dot{e} = -Ve + \chi + B_\sigma u_m - B_e \left(k_1 e + k_2 \text{sgn}(e)\right). \tag{12}$$

4.2 Torque Tracking Control

The rider's muscle groups track the generated desired torque trajectory via muscle stimulation within $q \in \mathcal{Q}_M$. The torque tracking error signal denoted by $e_\tau : \mathbb{R}_{\geq t_0} \to \mathbb{R}$ is designed based on the integral of the difference between the desired torque and the torque produced by the stimulated muscle contractions as

$$e_\tau \triangleq \int_{t_0}^{t} \left(\tau_d(\varphi) - \tau_a(\varphi)\right) d\varphi, \tag{13}$$

where the desired torque $\tau_d : \mathbb{R}_{\geq t_0} \to \mathbb{R}$ is bounded and periodic.

Remark 3. In (13), the desired torque trajectory τ_d is an explicit function of time. However, in the experiments in Section 6, the desired torque trajectory τ_d is a periodic function of the wrapped crank angle $q \in [0, 2\pi)$. Hence, a mapping between time and space is required. This mapping is feasible since there exists a relationship between time and the crank position. The angular speed of the system is defined as $\dot{q} \triangleq dq/dt$, which can be integrated to yield $q = \int_0^t \dot{q}(\varphi) d\varphi \triangleq f(t)$. This relationship between temporal and spatial coordinates is common for rotary machine systems as explained in Xu and Huang (2008). For the cycle-rider system, only forward pedaling is allowed and the desired cadence $\dot{q}_d$ is positive. Moreover, the cadence controller in (11) is designed and proven to achieve $\dot{q} > 0$ (i.e., the actual cadence is nonzero) based on the stability proof in Section 5. Hence, q is a strictly increasing function of t, (i.e., the relationship between t and q is bijective Xu and Huang (2008)). Thus the function $q = f(t)$ is analytic and the inverse function $t = f^{-1}(q)$ exists globally. Therefore, any function of t can also be expressed as a spatial function of q (e.g., $\tau_d(t)$ can be expressed as $\tau_d(f^{-1}(q))$).

The open-loop torque error system is obtained by taking the time derivative of (13) as

$$\dot{e}_\tau = \tau_d - B_\sigma u_m. \tag{14}$$

The muscle control input is designed as

$$u_m \triangleq \hat{W}_d + k_3 e_\tau - \nu_m, \tag{15}$$

where $k_3 \in \mathbb{R}_{>0}$ is a positive constant control gain, $\nu_m : \mathbb{R}_{\geq t_0} \to \mathbb{R}$ is a subsequently designed control input, and $\hat{W}_d : \mathbb{R}_{\geq t_0} \to \mathbb{R}$ is the subsequently designed repetitive learning control law.

Remark 4. The repetitive learning control law $\hat{W}_d(t)$ is typically designed based on the knowledge of the time period T of a periodic process Dixon et al. (2002); Sun et al. (2006). However, for the current development the implementable repetitive learning control law is designed based on the state-dependent desired torque trajectory τ_d. According to the mapping between time and space described in Remark 3, an implementable spatial repetitive learning law is denoted as $\hat{W}_d(t) = \hat{W}_d(f^{-1}(q))$. By defining the following map $q - 2\pi \triangleq f(t - T)$ and from the fact that q and $\dot{q}$ are measurable and positive, $\hat{W}_d(t - T) = \hat{W}_d(f^{-1}(q - 2\pi)$ can be obtained from the fact that $t - T = f^{-1}(q - 2\pi)$. Knowledge of the period T (i.e., the time to complete a revolution) is not necessary for the later implementation of $\hat{W}_d$, nevertheless it can be computed from $T = \int_{q-2\pi}^{q} dt = \frac{1}{\dot{q}} \int_{q-2\pi}^{q} dq$. The time period T depends on the cadence tracking performance and is expected to vary across crank cycles.

Based on the subsequent stability analysis and leveraging Remark 4, the repetitive learning control law in (15) is defined as

$$\begin{aligned} \hat{W}_d &\triangleq \Gamma \text{sat}_{\beta_r}\left(\hat{W}_d(t - T)\right) + k_L e_\tau, \\ &= \Gamma \text{sat}_{\beta_r}\left(\hat{W}_d(f^{-1}(q - 2\pi))\right) + k_L e_\tau. \end{aligned} \tag{16}$$

where $\Gamma \in (0, 1]$ is a selectable constant, $k_L \in \mathbb{R}_{>0}$ is a positive constant learning control gain, and $\text{sat}_{\beta_r}(\cdot)$ was previously defined in (6), and $\beta_r \in \mathbb{R}_{>0}$ is a selectable constant. The closed-loop error system is obtained by substituting (15) into (14) as

$$\dot{e}_\tau = \tilde{W}_d + \hat{W}_d - B_\sigma(\hat{W}_d + k_3 e_\tau - \nu_m), \tag{17}$$

where $\tilde{W}_d : \mathbb{R}_{\geq t_0} \to \mathbb{R}$ is the learning estimation error defined as $\tilde{W}_d \triangleq \tau_d - \hat{W}_d$. Based on the periodicity and boundedness of τ_d, $\tau_d(t) = \text{sat}_{\beta_r}(\tau_d(t)) = \text{sat}_{\beta_r}(\tau_d(t - T))$. Hence, by exploiting (16), the following expression can be developed

$$\tilde{W}_d = \text{sat}_{\beta_r}(\tau_d(t-T)) - \Gamma \text{sat}_{\beta_r}(\hat{W}_d(t-T)) - k_L e_\tau(t). \tag{18}$$

5. STABILITY ANALYSIS

The stability of the learning controller for torque tracking and robust sliding-mode controller for cadence tracking can be examined independently through the following two theorems. Theorem 1 shows that the closed-loop torque error system is output strictly passive and asymptotic tracking is achieved. Theorem 2 shows that the closed-loop cadence error system is output strictly passive and exponential tracking is achieved. In addition, Lemma 1 is included to prove that the time derivative of the torque tracking error in (13) is uniformly bounded.

Theorem 1. Given the closed-loop torque error system in (17), the system is output strictly passive (OSP) from input $v_1 \triangleq (1 + c_B)\hat{W}_d + c_b \nu_m$ to output e_τ when $q \in \mathcal{Q}_M$ and the controller designed in (15) and repetitive learning law in (16) ensures asymptotic tracking [1] in the sense that

$$\lim_{t \to \infty} e_\tau(t) = 0. \tag{19}$$

[1] For $q \notin \mathcal{Q}_M$ the torque controller in (15) and desired torque trajectory τ_d are zero.

Preprint submitted to 2nd IFAC Conference on Cyber-Physical & Human-Systems.
Received April 23, 2018.

Proof. Let $V_1 : \mathbb{R}^2 \times \mathbb{R}_{\geq t_0} \to \mathbb{R}$ be a nonnegative, continuously differentiable storage function defined as

$$V_1 \triangleq \frac{1}{2}e_\tau^2 + \frac{1}{2k_L}\int_{t-T}^{t} (\text{sat}_{\beta_r}(\tau_d(\varphi)) - \Gamma \text{sat}_{\beta_r}(\hat{W}_d(\varphi)))^2 d\varphi. \tag{20}$$

The storage function in (20) satisfies the following inequalities

$$\lambda_1 \|y\|^2 \leq V_1(y,t) \leq \lambda_2 \|y\|^2,$$

where $\lambda_1 \triangleq min(\frac{1}{2}, \frac{1}{2k_L})$, $\lambda_2 \triangleq max(\frac{1}{2}, \frac{1}{2k_L})$ and $y \triangleq [e_\tau \ \sqrt{Q_L}]^T$ where $Q_L \triangleq \int_{t-T}^{t}(\text{sat}_{\beta_r}(\tau_d(\varphi)) - \text{sat}_{\beta_r}(\hat{W}_d(\varphi)))^2 d\varphi$. Let $y(t)$ be a Filippov solution to the differential inclusion $\dot{y} \in K[h](y)$, where $K[\cdot]$ is defined as Filippov (1964) and h is defined by using (17) as $h \triangleq [h_1 \ h_2]$, where $h_1 \triangleq \tilde{W}_d + \hat{W}_d - B_\sigma(\hat{W}_d + k_3 e_\tau - \nu_m)$, $h_2 \triangleq \frac{1}{2\sqrt{Q_L}}\{(\text{sat}_{\beta_r}(\tau_d(t)) - \text{sat}_{\beta_r}(\hat{W}_d(t)))^2 - (\text{sat}_{\beta_r}(\tau_d(t-T)) - \text{sat}_{\beta_r}(\hat{W}_d(t-T)))^2\}$. The control input in (15) has the discontinuous lumped control effectiveness B_σ; hence the time derivative of (20) exists almost everywhere (a.e.), i.e., for almost all t. Based on Fischer et al. (2013, Lemma 1), $\dot{V}_1(y, t) \overset{a.e.}{\in} \dot{\tilde{V}}_1(y,t)$, where $\dot{\tilde{V}}_1$ is the generalized time derivative of (20) along the Filippov trajectories of $\dot{y} = h(y)$ and is defined as $\dot{\tilde{V}}_1 \triangleq \bigcap_{\xi \in \partial V_1} \xi^T K \left[\dot{e}_\tau \ \frac{\dot{Q}_L}{2\sqrt{Q_L}} \ 1\right]^T (e_\tau, 2\sqrt{Q_L}, t)$. Since $V_1(y,t)$ is continuously differentiable in y, $\partial V_1 = \{\nabla V_1\}$, thus

$$\dot{\tilde{V}}_1 \overset{a.e.}{\subset} [e_\tau, \ \left(\frac{1}{2k_L}\right) 2\sqrt{Q_L}] K \left[\dot{e}_\tau \ \frac{\dot{Q}_L}{2\sqrt{Q_L}}\right]^T. \tag{21}$$

Therefore, after substituting for (17), the generalized time derivative of (20) can be expressed as

$$\begin{aligned}\dot{\tilde{V}}_1 \overset{a.e.}{\subset} & e_\tau \left(\tilde{W}_d + \hat{W}_d - K[B_\sigma](k_3 e_\tau + \hat{W}_d - \nu_m)\right) \\ & - \frac{1}{2k_L}(\text{sat}_{\beta_r}(\tau_d(t-T)) - \text{sat}_{\beta_r}(\hat{W}_d(t-T)))^2 \\ & + \frac{1}{2k_L}(\text{sat}_{\beta_r}(\tau_d(t)) - \text{sat}_{\beta_r}(\hat{W}_d(t)))^2. \end{aligned} \tag{22}$$

By employing the following property Dixon et al. (2002)

$$\left(\tau_d(t) - \hat{W}_d(t)\right)^2 \geq \left(\text{sat}_{\beta_r}(\tau_d(t)) - \Gamma \text{sat}_{\beta_r}(\hat{W}_d(t))\right)^2,$$

using a similar proof as developed in Dixon et al. (2002, Appendix I), and using Property 6 to lower and upper bound $K[B_\sigma]$, using (18), and canceling terms, an upper bound for (22) can be developed as

$$\dot{\tilde{V}}_1 \overset{a.e.}{\leq} -\delta_1 e_\tau^2 + v_1 e_\tau, \tag{23}$$

where $v_1 = (1 + c_B)\hat{W}_d + c_b \nu_m$, $\delta_1 \triangleq c_b k_3 + \frac{k_L}{2}$, and $\delta_1 > 0$. Integrating (23) yields

$$\int_{t_0}^{t} v_1(\varphi) e_\tau(\varphi) d\varphi \overset{a.e.}{\geq} \left(\tilde{V}_1(t) - \tilde{V}_1(t_0) + \int_{t_0}^{t} \delta_1 e_\tau^2(\varphi) d\varphi\right). \tag{24}$$

Hence, the system is output strictly passive (OSP) from the input v_1 to the output e_τ. Therefore, the closed-loop system in (17) is passive with a radially unbounded positive definite storage function. From Sepulchre et al. (1997, Theorem 2.28), to prove asymptotic tracking, the zero-state observability condition has to be satisfied [2]. By designing ν_m in (15) as $\nu_m \triangleq -k_4 \hat{W}_d$, where $k_4 \triangleq \frac{\gamma_1}{c_b}$, and substituting it into (23), $\dot{\tilde{V}}_1 \overset{a.e.}{\leq} -\delta_1 e_\tau^2 \leq 0$. By invoking Fischer et al. (2013, Corollary 2) and since $\dot{\tilde{V}}_1(y, t) \overset{a.e.}{\leq} -W(y)$, where W is a continuous positive semi-definite function, $|e_\tau| \to 0$ as $t \to \infty$. Since $V_1 \geq 0$ and $\dot{V}_1 \overset{a.e.}{\leq} 0$, $V_1 \in \mathcal{L}_\infty$, hence, $e_\tau, Q_L \in \mathcal{L}_\infty$. From (16), $\hat{W}_d \in \mathcal{L}_\infty$, which along with the fact that $\tau_d \in \mathcal{L}_\infty$, implies that $\tilde{W}_d \in \mathcal{L}_\infty$. From (15), $u_m \in \mathcal{L}_\infty$. Hence the closed-loop system in (17) is passive and asymptotic tracking is achieved.

Lemma 1. The torque tracking error $\dot{e}_\tau$ in (17) is uniformly bounded for $q \in \mathcal{Q}_M$ in the sense that

$$\begin{aligned}|\dot{e}_\tau| \leq & \left(2 + c_B\left(1 + \frac{k_3}{k_L} + k_4\right)\right) k_L |e_\tau| \\ & + \left(2 + \frac{1}{\Gamma} + c_B(1 + k_4)\right)\Gamma \beta_r. \end{aligned} \tag{25}$$

Proof. The expression in (25) is a direct result of Theorem 1 obtained by analyzing (17); since $e_\tau, \hat{W}_d, \tilde{W}_d \in \mathcal{L}_\infty$, $\dot{e}_\tau \in \mathcal{L}_\infty$.

Theorem 2. Given the closed loop error system in (12), the system is output strictly passive (OSP) from input $v_2 \triangleq B_\sigma u_m$ to output e and achieves exponential tracking when $u_m = 0$, provided the following sufficient gain conditions are satisfied

$$k_1 > \frac{c_2}{c_e}, \ \ k_2 > \frac{c_1}{c_e}. \tag{26}$$

Proof. Let $V_2 : \mathbb{R} \times \mathbb{R}_{\geq t_0} \to \mathbb{R}$ be a nonnegative, continuously differentiable, storage function defined as

$$V_2 = \frac{1}{2} M e^2. \tag{27}$$

The storage function in (27) satisfies the following inequalities

$$\lambda_3 |e|^2 \leq V_2(e,t) \leq \lambda_4 |e|^2,$$

where $\lambda_3 \triangleq \frac{c_m}{2}$, $\lambda_4 \triangleq \frac{c_M}{2}$. Let $e(t)$ be a Filippov solution to the differential inclusion $\dot{e} \in K[h_3](e)$, where $K[\cdot]$ is defined as in Fischer et al. (2013), and h_3 is defined using (7) as $h_3 \triangleq M^{-1}\{-Ve + \chi + B_\sigma u_m - B_e(k_1 e - k_2 sgn(e))\}$. Using similar arguments as in the proof of Theorem 1, and using (10), (12), and Properties 5 and 6, the generalized time derivative of (27) can be upper bounded as

$$\dot{\tilde{V}}_2 \overset{a.e.}{\leq} -(k_1 c_e - c_2) e^2 - (k_2 c_e - c_1)|e| + (B_\sigma u_m) e. \tag{28}$$

Integrating and upper bounding (28) yields

$$\int_{t_0}^{t} v_2(\varphi) e(\varphi) d\varphi \overset{a.e.}{\geq} (\tilde{V}_2(t) - \tilde{V}_2(t_0) + \int_{t_0}^{t} \delta_2 \|e(\varphi)\|^2 d\varphi), \tag{29}$$

[2] In Sadikhov and Haddad (2014), the definition of zero-state observability is described for Filippov solutions.

Preprint submitted to 2nd IFAC Conference on Cyber-Physical & Human-Systems.
Received April 23, 2018.

where $\delta_2 = k_1 c_e - c_2$, and $v_2 = B_\sigma u_m$, which can be used to prove that the closed-loop system in (12) is output strictly passive (OSP) from input v_2 to output e, provided the gain conditions in (26) are satisfied. Moreover, $\dot{V}_2 \overset{a.e.}{\leq} -\delta_2 V_2$ when $q \notin \mathcal{Q}_M$ since $\sigma_m = 0 \implies B_\sigma = 0, \forall m \in \mathcal{M}$, provided the gain conditions in (26) are satisfied. Hence, exponential cadence tracking is obtained in the sense that

$$\|e(t)\| \leq \sqrt{\frac{\lambda_4}{\lambda_3}} \|e(t_n)\| \exp\left(-\frac{\delta_2}{2}(t - t_n)\right), \forall q \notin \mathcal{Q}_M.$$

6. EXPERIMENTS

The cadence controller designed in (11) and torque controller in (15) with the learning-based feedforward control term in (16) were tested in an experiment on one healthy female (aged 24). The switched muscle control input was commanded as stimulation intensities u_m to activate the right and left quadriceps used for torque tracking, and as current input u_e to the electric motor for cadence tracking. Prior to participation, written informed consent was obtained from the participant, as approved by the Institutional Review Board at the University of Florida. The participant was instructed to avoid voluntarily contributing to pedaling and no feedback was provided regarding the tracking performance during the experiment.

6.1 Experimental Setup

The motorized recumbent tricycle described in Bellman et al. (2017); Duenas et al. (to appear) with crank position (using an US Digital optical encoder) and torque (using a SRM Science Road Wireless Power Meter) feedback was used for the FES cycling experiments.The stimulation current amplitudes and frequency were selected as 90 mA and 60 Hz, respectively. Initial measurements of the participant's lower extremities were recorded as in Bellman et al. (2016) to determine the stimulation pattern (i.e., the crank positions where the muscle groups were electrically stimulated).

The FES cycling trial had a duration of $t_d = 120$ seconds. The experiment started with the electric motor tracking a steady state cadence of 45 RPM. When the experiment duration reached $t_1 = 20$ seconds, the ESC algorithm in (5) began modifying the desired cadence $\dot{q}_d$ and desired torque τ_d (by modulating the peak torque demand). Also at t_1, the torque controller in (15) was activated (i.e., the lower-limb muscles were stimulated). Due to the importance of the knee joint torque for torque generation to the crank Fregly and Zajac (1996), the desired torque trajectory was designed to be a modified function of the knee joint torque transfer ratio, (which can be computed as a function of the crank angle and anatomical lengths of the rider). Hence, the desired torque trajectory is periodic based on the crank angle and nonzero during the stimulation regions (i.e., for $q \in \mathcal{Q}_M$) and is defined in (30), where $q_1, q_2, q_3, q_4 \in \mathbb{R}_{>0}$ are constant predefined crank angles within $q \in \mathcal{Q}_M$ representing the starting and ending crank positions of the stimulation regions of the rider, and the peak torque amplitude $A_d \in \mathbb{R}_{\geq 0}$ was computed by the ESC algorithm in (5). The ESC parameters introduced in (5) were selected for generating $\dot{q}_d$ as $\omega \triangleq 0.5$, $\alpha_p \triangleq 0.1$, $k_d \triangleq 0.1$, $k_\theta \triangleq 0.25$, and $k_h \triangleq 0.08$ and for generating τ_d (i.e., for the peak torque demand A_d) as $\omega \triangleq 0.01$, $\alpha_p \triangleq 1$, $k_d \triangleq 01$, $k_\theta \triangleq 0.65$, and $k_h \triangleq 0.25$. The control gains introduced in (11), (15), and (16) were selected as follows: $k_m \triangleq 1$, $k_1 \triangleq 9$, $k_2 \triangleq 0.2$, $k_3 \triangleq 55$, $k_4 \triangleq 0.1$, $\Gamma \triangleq 0.9$, and $k_L \triangleq 5$. The initial conditions of the ESC parameters in (5) for generating $\dot{q}_d$ were selected as $\hat{\theta} \triangleq 45$ RPM (initial cadence that the motor tracked during the first 20 seconds of the experiments), $\nu = \frac{\text{sat}(P_a)}{k_h}$, and $w \triangleq 0$; and for τ_d the parameters were selected as $\hat{\theta} = 1$ N·m, $\nu = \frac{\text{sat}(P_a)}{k_h}$, and $w \triangleq 0$.

6.2 Results

Figure 1 illustrates the computed desired cadence trajectory and the peak torque demand by the ESC algorithm in (5). Figure 2 shows the cadence tracking error $\dot{e}$ and the torque tracking error $\dot{e}_\tau$. Figure 3 depicts the stimulation intensities delivered to the muscle groups u_m, the electric motor current input u_e, and the learning control input $\hat{W}_d$. The stimulation intensities were saturated at 100μs as seen in Figure 3 for subject comfort. The peak torque demand in Figure 1 increases to make the rider evoke a higher torque output, which results in an increase in the stimulation intensities delivered to the quadriceps muscle groups in Figure 3. Cadence tracking is regulated within a range of ±5 RPM from the desired cadence computed by the ESC algorithm.

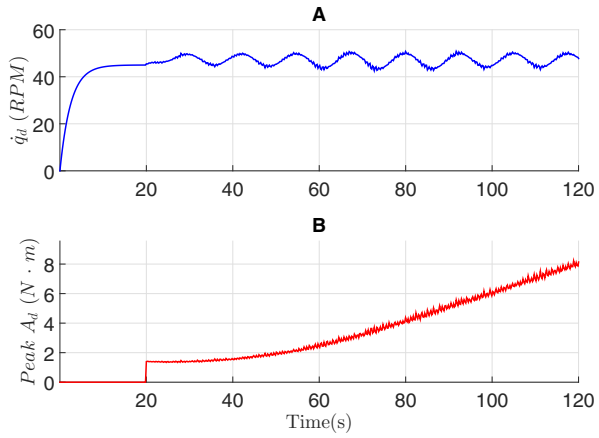

Fig. 1. Desired cadence trajectory $\dot{q}_d$ (A) and maximum torque demand A_d (B) computed by the ESC algorithm.

7. CONCLUSION

An ESC algorithm was implemented to determine optimal cadence and torque tracking trajectories during an FES-cycling protocol. The ESC algorithm calculated the desired cadence trajectory and the peak torque demand. A cadence controller was designed to command current to the electric motor and a torque controller to command stimulation intensities to the quadriceps muscle groups to achieve power tracking. The switched muscle torque controller included a feedforward learning input that compensated for the periodic dynamics of the desired torque

Preprint submitted to 2nd IFAC Conference on Cyber-Physical & Human-Systems.
Received April 23, 2018.

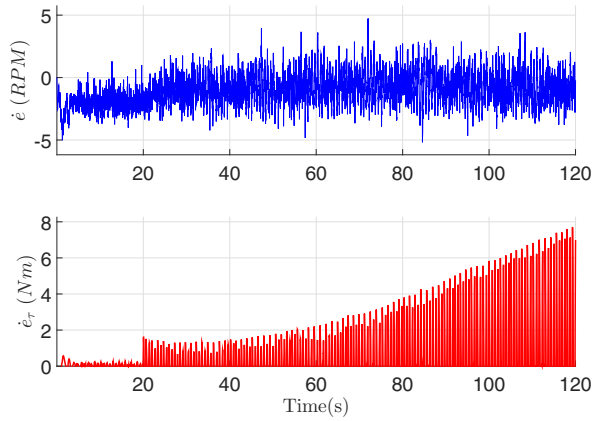

Fig. 2. Tracking performance quantified the cadence tracking error $\dot{e}$ (A) and the torque tracking error $\dot{e}_\tau$ (B).

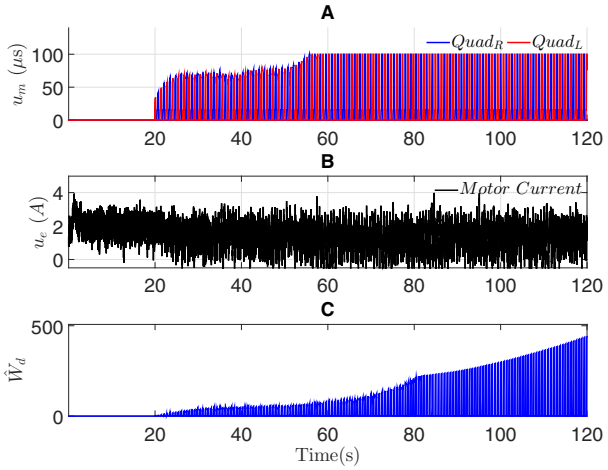

Fig. 3. Stimulation intensities delivered to the quadriceps muscle groups denoted by u_m for each muscle (A), the electric motor current input u_e (B) and the learning control input $\hat{W}_d$ in (C).

trajectory. A passivity-based analysis was developed to ensure stability of the torque and cadence closed-loop systems. Future work includes extended FES-cycling experiments with people with movement disorders, where tracking comparisons can be made based on the selection of different parameters of the ESC algorithm.

REFERENCES

Ariyur, K.B. and Krstic, M. (2003). *Real-Time Optimization by Extremum-Seeking Control*. Wiley.

Beckerle, P., Salvietti, G., Unal, R., Prattichizzo, D., Rossi, S., Castellini, C., Hirche, S., Endo, S., Amor, H.B., Ciocarlie, M., Mastrogiovanni, F., Argall, B.D., and Bianchi, M. (2017). A human-robot interaction perspective on assistive and rehabilitation robotics. *Frontiers in Neurorobotics*, 11(24).

Bellman, M. (2015). *Control of Cycling Induced by Functional Electrical Stimulation: A Switched Systems Theory Approach*. Ph.D. thesis, University of Florida.

Bellman, M.J., Cheng, T.H., Downey, R.J., Hass, C.J., and Dixon, W.E. (2016). Switched control of cadence during stationary cycling induced by functional electrical stimulation. *IEEE Trans. Neural Syst. Rehabil. Eng.*, 24(12), 1373–1383.

Bellman, M.J., Downey, R.J., Parikh, A., and Dixon, W.E. (2017). Automatic control of cycling induced by functional electrical stimulation with electric motor assistance. *IEEE Trans. Autom. Science Eng.*, 14(2), 1225–1234. doi:10.1109/TASE.2016.2527716.

Bo, A.P.L., Fonseca, L., Guimaraes, J., Fachin-Martins, E., Paredes, M.E.G., Brindeiro, G.A., de Sousa, A.C.C., Dorado, M.C., and Ramos, F. (2017). Cycling with spinal cord injury: A novel system for cycling using electrical stimulation for individuals with paraplegia, and preparation for cybathlon 2016. *Robot Autom. Mag.*, 24(4), 58–65.

Cao, Z., Dürr, H.B., Ebenbauer, C., Allgöwer, F., and Gao, F. (2017). Iterative learning and extremum seeking for repetitive time-varying mappings. *IEEE Trans. Autom. Contol*, 62(7), 3339–3353.

Chen, S., Wang, L., Ma, K., and Zhao, H. (2017). A switching-based extremum seeking control scheme. *International Journal of Control*, 90(8), 1688–1702.

Cousin, C., Duenas, V.H., Rouse, C., and Dixon, W.E. (2017). Motorized functional electrical stimulation for torque and cadence tracking: A switched lyapunov approach. In *Proc. IEEE Conf. Decis. Control*, 5900–5905.

Dixon, W.E., Zergeroglu, E., Dawson, D.M., and Costic, B.T. (2002). Repetitive learning control: A lyapunov-based approach. *IEEE Trans. Syst. Man Cybern. Part B Cybern.*, 32, 538–545.

Duenas, V., Cousin, C., Parikh, A., and Dixon, W.E. (2016). Functional electrical stimulation induced cycling using repetitive learning control. In *Proc. IEEE Conf.*

$$\tau_d(q) \triangleq \begin{cases} A_d \sin\left(2\frac{q-q_1}{\frac{1}{2}q_2-q_1}\pi\right) & q_1 < q \leq \frac{1}{2}q_2 \\ \frac{A_d}{2}\cos\left(\frac{q-\frac{1}{2}q_2}{\frac{1}{2}q_2}\pi\right)+\frac{A_d}{2} & \frac{1}{2}q_2 < q \leq q_2 \\ 0 & q_2 < q \leq q_3 \\ A_d \sin\left(\frac{q-q_3}{q_4-q_3}\pi\right) & q_3 < q \leq \frac{q_4+q_3}{2} \\ \frac{A_d}{2}\cos\left(\frac{q-\frac{1}{2}(q_4-q_3)+q_3}{\frac{1}{2}(q_4-q_3)}\pi\right)+\frac{A_d}{2} & \frac{q_3+q_4}{2} < q \leq q_4 \\ 0 & q_4 < q \leq q_1 \end{cases}, \tag{30}$$

Preprint submitted to 2nd IFAC Conference on Cyber-Physical & Human-Systems.
Received April 23, 2018.

Decis. Control.

Duenas, V.H., Cousin, C.A., Parikh, A., Freeborn, P., Fox, E.J., and Dixon, W.E. (to appear). Motorized and functional electrical stimulation induced cycling via switched repetitive learning control. *IEEE Trans. Control Syst. Tech.*

Farhoud, A. and Erfanian, A. (2014). Fully automatic control of paraplegic FES pedaling using higher-order sliding mode and fuzzy logic control. *IEEE Trans. Neural Syst. Rehabil. Eng.*, 22(3), 533–542. doi: 10.1109/TNSRE.2013.2296334.

Ferrante, S., Pedrocchi, A., Ferrigno, G., and Molteni, F. (2008). Cycling induced by functional electrical stimulation improves the muscular strength and the motor control of individuals with post-acute stroke. *Eur. J. Phys. Rehabil. Med.*, 44(2), 159–167.

Filippov, A.F. (1964). Differential equations with discontinuous right-hand side. In *Fifteen papers on differential equations*, volume 42 of *American Mathematical Society Translations - Series 2*, 199–231. American Mathematical Society.

Fischer, N., Kamalapurkar, R., and Dixon, W.E. (2013). LaSalle-Yoshizawa corollaries for nonsmooth systems. *IEEE Trans. Autom. Control*, 58(9), 2333–2338.

Fregly, B.J. and Zajac, F.E. (1996). A state-space analysis of mechanical energy generation, absorption, and transfer during pedaling. *J. Biomech.*, 29(1), 81–90.

Guay, M. (2016). A perturbation-based proportional integral extremum-seeking control approach. *IEEE Trans. Autom. Contol*, 61(11), 3370–3381.

Hunt, K.J., Stone, B., Negård, N.O., Schauer, T., Fraser, M.H., Cathcart, A.J., Ferrario, C., Ward, S.A., and Grant, S. (2004). Control strategies for integration of electric motor assist and functional electrical stimulation in paraplegic cycling: Utility for exercise testing and mobile cycling. *IEEE Trans. Neural Syst. Rehabil. Eng.*, 12(1), 89–101.

Kawai, H., Bellman, M., Downey, R., and Dixon, W.E. (to appear). Closed-loop position and cadence tracking control for FES-cycling exploiting pedal force direction with antagonistic bi-articular muscles. *IEEE Trans. Control Syst. Tech.*

Khalil, H.K. (2002). *Nonlinear Systems*. Prentice Hall, Upper Saddle River, NJ, 3 edition.

Killingsworth, N.J. and Krstic, M. (2006). PID tuning using extremum seeking: online, model-free performance optimization. *IEEE Control Syst. Mag.*, 26(1), 70–79.

Koropouli, V., Gusrialdi, A., Hirche, S., and Lee, D. (2016). An extremum-seeking control approach for constrained robotic motion tasks. *Control Eng. Pract.*, 52, 1–14.

Krstic, M. and Wang, H.H. (2000). Stability of extremum seeking feedback for general nonlinear dynamic systems. *Automatica*, 36(4), 595–601.

Moura, S.J. and Chang, Y.A. (2010). Asymptotic convergence through lyapunov-based switching in extremum seeking with application to photovoltaic systems. In *Proc. Am. Control Conf.*, 3542–3548.

Nataraj, R., Audu, M.L., and Triolo, R.J. (2017). Restoring standing capabilities with feedback control of functional neuromuscular stimulation following spinal cord injury. *Med. Eng. Phys.*, 42, 13–25.

Oliveira, T.R., Costa, L.R., and Pino, A.V. (2016). Extremum seeking applied to neuromuscular electrical stimulation. *IFAC-PapersOnLine*, 49(32), 188–193.

Poveda, J.I. and Teel, A.R. (2017). A framework for a class of hybrid extremum seeking controllers with dynamic inclusions. *Automatica*, 76, 113–126.

Poveda, J.I., Vamvoudakis, K.G., and Benosman, M. (2017). A neuro-adaptive architecture for extremum seeking control using hybrid learning dynamics. In *Proc. Am. Control Conf.*, 542–547.

Rahnama, A., Xia, M., Wang, S., and Antsaklis, P.J. (2016). Passivation and performance optimization using an extremum seeking co-simulation framework with application to adaptive cruise control systems. In *Proc. Am. Control Conf.*, 6109–6114.

Sadikhov, T. and Haddad, W.M. (2014). On the equivalence between dissipativity and optimality of discontinuous nonlinear regulator for filippov dynamical systems. *IEEE Trans. Autom. Contol*, 59(5), 423–436.

Sadowsky, C.L., Hammond, E.R., Strohl, A.B., Commean, P.K., Eby, S.A., Damiano, D.L., Wingert, J.R., Bae, K.T., and John W. McDonald, I. (2013). Lower extremity functional electrical stimulation cycling promotes physical and functional recovery in chronic spinal cord injury. *J. Spinal Cord Med.*, 36(6), 623–631.

Sepulchre, R., Janković, M., and Kokotović, P.V. (1997). *Constructive Nonlinear Control*. New York: Springer-Verlag.

Stegath, K., Sharma, N., Gregory, C., and Dixon, W.E. (2007). An extremum seeking method for non-isometric neuromuscular electrical stimulation. In *Proc. IEEE Int. Conf. Syst. Man Cybern.*, 2528–2532. Montréal, Canada.

Sun, M., Ge, S.S., and Mareels, I.M. (2006). Adaptive repetitive learning control of robotic manipulators without the requirement for initial repositioning. *IEEE Trans. Robot.*, 22(3), 563–568.

Szecsi, J., Straube, A., and Fornusek, C. (2014). Comparison of the pedalling performance induced by magnetic and electrical stimulation cycle ergometry in able-bodied subjects. *Med. Eng. Phys.*, 36(4), 484–489. doi: 10.1016/j.medengphy.2013.09.010.

Xu, J.X. and Huang, D. (2008). Spatial periodic adaptive control for rotary machine systems. *IEEE Trans. Autom. Control*, 53(10), 2402–2408.

Ye, M. and Hu, G. (2016). Distributed extremum seeking for constrained networked optimization and its application to energy consumption control in smart grid. *IEEE Trans. Control Syst. Technol.*, 24(6), 2048–2058.

Zhang, C. and nez, R.O. (2009). Robust and adaptive design of numerical optimization-based extremum seeking control. *Automatica*, 45(3), 634–646.

Zhang, J., Cheah, C.C., and Collins, S.H. (2015). Experimental comparison of torque control methods on an ankle exoskeleton during human walking. In *Proc. IEEE Int. Conf. Robot. Autom.*, 5584–5589. doi: 10.1109/ICRA.2015.7139980.

Zhang, X.T., Dawson, D.M., Dixon, W.E., and Xian, B. (2006). Extremum seeking nonlinear controllers for a human exercise machine. *IEEE Trans. Mechatron.*, 11, 233–240. URL `http://ncr.mae.ufl.edu/papers/mech06.pdf`.

Preprint submitted to 2nd IFAC Conference on Cyber-Physical & Human-Systems.
Received April 23, 2018.